Physics Letters B 666 (2008) 222–227

Contents lists available at ScienceDirect

Physics Letters B

www.elsevier.com/locate/physletb

Lifetime measurements of excited states in ^{17}C: Possible interplay between collectivity and halo effects

D. Suzuki [a,*], H. Iwasaki [a,1], H.J. Ong [a,b,2], N. Imai [b,3], H. Sakurai [b,a], T. Nakao [a], N. Aoi [b], H. Baba [b], S. Bishop [b], Y. Ichikawa [a,4], M. Ishihara [b], Y. Kondo [c,4], T. Kubo [b], K. Kurita [d], T. Motobayashi [b], T. Nakamura [c], T. Okumura [c], T.K. Onishi [a], S. Ota [e], M.K. Suzuki [a], S. Takeuchi [b], Y. Togano [d], Y. Yanagisawa [b]

[a] Department of Physics, University of Tokyo, 7-3-1 Hongo, Bunkyo, Tokyo 113-0033, Japan
[b] RIKEN, Nishina Center, 2-1 Hirosawa, Wako, Saitama 351-0198, Japan
[c] Department of Physics, Tokyo Institute of Technology, 2-12-1 Ookayama, Meguro, Tokyo 152-8551, Japan
[d] Department of Physics, Rikkyo University, 3-34-1 Nishi-Ikebukuro, Toshima, Tokyo 171-8501, Japan
[e] CNS, University of Tokyo, RIKEN Campus, 2-1 Hirosawa, Wako, Saitama 351-0198, Japan

ARTICLE INFO

Article history:
Received 6 December 2007
Received in revised form 21 May 2008
Accepted 11 July 2008
Available online 16 July 2008
Editor: D.F. Geesaman

PACS:
23.20.Js
21.10.Tg
27.20.+n
29.30.Kv

ABSTRACT

Lifetime measurements were performed on low-lying excited states of the neutron-rich isotope ^{17}C using the recoil shadow method. The γ-decay mean lifetimes were determined to be $583 \pm 21(\text{stat}) \pm 35(\text{syst})$ ps for the first excited state at 212 keV and $18.9 \pm 0.6(\text{stat}) \pm 4.7(\text{syst})$ ps for the second excited state at 333 keV. Based on a comparison with the empirical upper limits for the electromagnetic transition strengths, these decays are concluded to be predominantly M1 transitions. The reduced M1 transition probabilities to the ground state were deduced to be $(1.0 \pm 0.1) \times 10^{-2}\mu_N^2$ and $(8.2^{+3.2}_{-1.8}) \times 10^{-2}\mu_N^2$, respectively, for the first and second excited states. The strongly hindered M1 strength as well as the lowered excitation energy represents unique nature of the 212-keV state.

In recent years neutron-rich carbon isotopes have attracted much attention because of their unique properties rarely encountered in stable nuclei. In particular, manifestation of collectivity may be one of the prevailing features for these isotopes. Indeed, recent studies with proton inelastic scattering have revealed fairly large deformation lengths for excitations of ^{16}C [1] and ^{17}C [2]. For the case of ^{16}C, however, a suppressed proton quadrupole collectivity has been suggested by the E2 strength observed for the transition between the ground 0^+ and first 2^+ states [3,4], and further examined by the successive experimental studies [5,6]. To account for such behaviors of C isotopes, several theoretical studies have been carried out, predicting plausible phenomena such as the occurrence of opposite shapes of deformation between protons and neutrons [7] or a shape transition from prolate to oblate deformation as one approaches the neutron-drip line [8]. Another important aspect for the isotopes near the neutron drip line is the emergence of halo structure, as clearly observed in ^{19}C [9]. This phenomenon is ascribed to the spatial extension of the valence neutron distribution, enhanced by tunneling through the nuclear potential well. Hence, weakly-bound *s*-wave neutrons are most responsible for such phenomenon.

Among the neutron-rich carbon isotopes, the weakly-bound carbon isotope ^{17}C, with $N = 11$, may present an intriguing case where one can anticipate cooperative effects between collectivity and halo structure. As a matter of fact, the low-lying level scheme of ^{17}C exhibits a couple of unique features. Firstly, the spin-parity of the ground state is found to be $3/2^+$ as confirmed by the measurements of the β-decay branching ratio [10] and the g-factor [11]. The results from the studies using one-neutron knockout [12–15] and Coulomb breakup [16] of ^{17}C are also in harmony with the spin-parity of $3/2^+$ for the ground state. This assignment, however, is in contradiction with the naive shell model expectation that the ground state of an odd nucleus with $N = 11$ should have the spin-parity of $5/2^+$. On the other hand, a theoretical study in terms of mean-field calculation suggests a subtle competition among the $1/2^+$, $3/2^+$ and $5/2^+$ states, where the $3/2^+$ state tends to be most lowered when prolate deformation dominates [8].

Secondly, a recent work of in-beam γ-ray spectroscopy using two-step fragmentation [17] revealed two bound excited states lo-

* Corresponding author.
E-mail address: dsuzuki@nucl.phys.s.u-tokyo.ac.jp (D. Suzuki).
[1] Present address: Institut für Kernphysik, Universität zu Köln, Germany.
[2] Present address: RCNP, Osaka University, Mihogaoka 10-1, Ibaraki, Osaka 567-0047, Japan.
[3] Present address: RIKEK, 1-1 Oho, Tsukuba, Ibaraki 305-0801, Japan.
[4] Present address: RIKEN, Nishina Center, 2-1 Hirosawa, Wako, Saitama 351-0198, Japan.

0370-2693
doi:10.1016/j.physletb.2008.07.055

cated below the very low neutron emission threshold (S_n) at about 730 keV [18]. These states are almost degenerate with excitation energies of about 220 keV and 330 keV, respectively, both deexciting directly to the ground state. The spin-parity of the second excited state has recently been confirmed to be $5/2^+$ [19], while a tentative assignment of $1/2^+$ was made for the first excited state [2,19]. It is possible that the first excited state, with the plausible assignment of $1/2^+$, may form a halo structure because of the small binding energy involved. Indeed, an anomalous feature of the first excited state was indicated in a study using proton inelastic scattering [2], where a much smaller excitation strength was found for this state as compared to that for the second excited state.

To gain further insight into the underlying nuclear structure, information on the electromagnetic transition strengths should be useful. In particular, if the tentative spin assignments are correct, the γ-decays to the $3/2^+$ ground state are expected to be predominantly M1 transitions. The M1 strengths observed could then afford sensitive probes to the characteristic behaviors of valence neutrons in the initial and final states. The lifetime measurement is particularly useful for extracting M1 strengths while other methods such as using nuclear reactions can hardly determine the M1 strength independently of theoretical models. Coulomb excitation method affords an exceptional case by allowing theoretically unambiguous determination of electromagnetic transition strengths. However, this method is less sensitive to magnetic multipole transitions, often hiding M1 components under favorably excited E2 components.

In the present Letter, we report on lifetime measurements conducted for the first and second excited states of ^{17}C. From the mean lifetimes (τ) observed, the electromagnetic transition strengths were determined for the corresponding γ deexcitations. The lifetime measurements were performed by employing the recoil shadow method (RSM) with intermediate-energy radioactive-isotope beams [3], which may allow determination of lifetimes from nano- to low pico-second range. In this method, the lifetime is obtained by observing the angular distribution of γ rays emitted from excited ^{17}C nuclei in flight. This angular distribution is a function of the distribution of emission points of γ rays, which is in turn governed by the lifetime. In reality, the resultant shift in the angular distribution is only marginal for the lifetimes in the region of pico-seconds since the flight distance is so short, of the order of 1 mm, even for swiftly moving nuclei with intermediate-energies. In order to facilitate measurement of such short lifetimes, a lead shield is incorporated to be placed close to the target. The attenuation of the γ rays through the shield sharply varies as a function of emission point and thus provides a strong lifetime dependence for the γ-ray angular distribution.

This method was first employed in our earlier work on ^{16}C [3]. In the present work, the method was upgraded further to gain efficiency and precision by taking the following measures: firstly, the number of NaI(Tl) detectors was increased from 32 to 130, resulting in a larger coverage of the solid angle. Secondly, measurements of the angular distributions were carried out both with and without the lead shield. Comparison of the pair of data then served to remove possible disturbing effects from intrinsic anisotropies of γ-ray emissions caused by the reaction mechanism. In practice, we introduce a new quantity, the deficiency of the γ-ray yield, which is defined as the yield ratio between the pair of measurements taken for the detectors at a given angle. This quantity, which represents the shadow effect of the lead shield, is almost free from the intrinsic γ-ray anisotropy thanks to the cancellation between the numerator and denominator. More details on the improved RSM are found in Ref. [6].

Another important aspect for a successful application of the RSM concerns a proper choice of the reaction which can favorably populate the states of interest. This is particularly important for the case of odd nuclei where low-lying level schemes are relatively complicated and disordered. In the present study, the break-up reaction of ^{18}C, at 79 A MeV, on a ^{9}Be target was proved efficiently to populate the two excited states of ^{17}C, while inelastic scatterings may not be preferable because of small population expected for the first excited state [2].

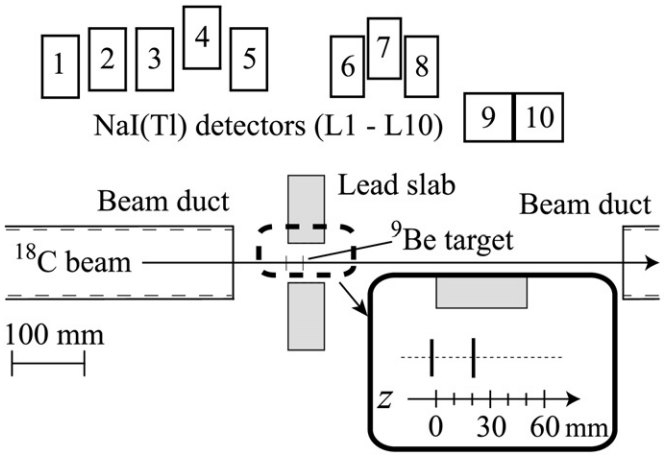

Fig. 1. Schematic view of the experimental setup. A ^{9}Be target was surrounded by ten layers of NaI(Tl) detectors (L1–L10) to detect deexcitation γ rays from ^{17}C. A lead slab was used as the γ-ray shield. Two different target positions at $z = 20.5$ mm (the center target position) and -1.5 mm (the upstream target position) were employed.

The experiment was performed at the RIKEN Accelerator Research Facility using a ^{18}C secondary beam provided from the RIKEN Projectile-fragment Separator (RIPS) [20]. The secondary beam was produced in projectile fragmentation reactions of 110-A MeV ^{22}Ne primary ions impinging on a 1.02-g/cm^2 ^{9}Be production target with a typical beam intensity of 320 pnA. Particle identification of the secondary beam was performed on an event-by-event basis by means of the TOF-ΔE method using two 1.0-mm thick plastic scintillation counters, placed 5.1 m apart along the beam line. The ^{18}C secondary beam had a typical intensity of 2.3×10^4 counts per second with a purity of about 60%, and was directed onto a 370-mg/cm^2 ^{9}Be reaction target set at the final focal plane of RIPS. Positions and incident angles of the secondary beam particles were recorded with two sets of parallel plate avalanche counters (PPACs) [21] placed upstream of the reaction target. Outgoing particles were detected by a plastic scintillator hodoscope [22], located 3.8 m downstream of the target, facilitating particle identification with the TOF-ΔE–E method. The scattering angle of the particle was determined by combining the hit position on the hodoscope with those on the PPACs for the incoming particles.

Fig. 1 shows a schematic view of the setup employed in the present experiment. A large array of 130 NaI(Tl) detectors, divided into ten separate layers (labeled L1–L10), surrounded the target to detect deexciting γ rays. The L1–L8 layers consisted of 98 detectors, which are part of DALI2 [23], while the L9 and L10 layers consisted of 32 detectors from DALI [24]. In each layer, the detectors were placed cylindrically to take nearly the same polar angle with respect to the beam direction. Energy thresholds of the detectors were set to 150–200 keV for γ rays in the projectile frame.

To serve for the γ-ray shield, a 5 cm-thick lead slab was installed between the L5 and L6 layers. The slab had an area of 24×24 cm^2 with a 5.4-cm diameter hole in the center. In the present work, γ-ray measurements were performed for two different target positions along the beam axis (z-axis), i.e., the "center target position" of $z = 20.5$ mm and the "upstream target position" of $z = -1.5$ mm, where the origin ($z = 0$) is taken as the

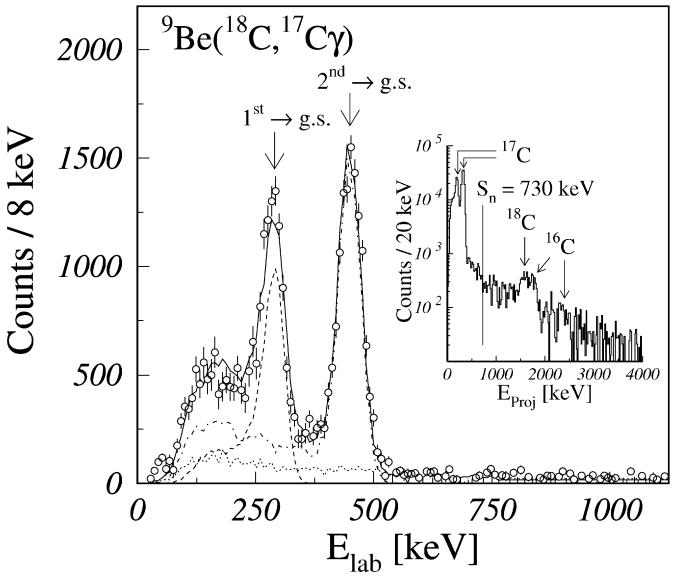

Fig. 2. The γ-ray energy spectrum, in the laboratory frame, obtained in coincidence with outgoing ^{17}C particles. The data are denoted by the open circles with the error bars. The result of a fit to the spectrum is shown by the solid curve, which includes the simulated spectra for the 212-keV (dashed) and 333-keV (dot-dashed) γ rays and the ^{14}C spectrum (dotted) as a background. The two prominent peaks indicated by the arrows correspond to the 212-keV and 333-keV transitions. The inset shows the γ-ray energy spectrum, in the projectile frame, measured in the entire NaI(Tl) array.

upstream edge of the lead slab. The reaction target was placed in the air outside the beam duct. Hence we also made a supplementary measurement without the target to estimate the background due to reactions with materials such as the air along the beam line.

To find efficiencies and response functions of the NaI(Tl) detectors under the given experimental conditions, a simulation with the Monte Carlo code, GEANT [25], was performed by incorporating parameters for the employed geometries of the setup. The validity of the simulation was then tested using the data taken with ^{22}Na, ^{60}Co and ^{137}Cs standard sources, placed at five different positions between $z = -1.5$ and 51.5 mm. For the respective target positions, the data were taken with and without the lead shield. Taking the yield ratio of the γ rays in the full-energy-peak between these two measurements, the deficiency (D) was deduced for the cluster of NaI(Tl) detectors belonging to each layer. The simulation reproduced the measured deficiencies with accuracies of $\pm 3\%$ and $\pm 7\%$ for the layers with $D \geqslant 0.2$ and with $D < 0.2$, respectively.

Fig. 2 shows a typical energy spectrum of γ rays, in the laboratory frame, measured in coincidence with outgoing ^{17}C particles. This spectrum was obtained with the detectors in the L10 layer when the target was placed at the position of the upstream setup without the lead shield. One-fold events in the entire NaI(Tl) array were selected to improve the peak-to-Compton ratio. In addition, a gate was imposed on the timing spectrum of the NaI(Tl) detectors to select prompt events. The accidental coincidences with the natural background γ radiation were evaluated with the energy spectrum obtained outside the prompt time gate, and were subtracted. Using the data taken without the target, a further subtraction was performed for the beam-induced background that came from materials other than the target.

In Fig. 2, two prominent peaks are clearly observed. Taking into account the Doppler effect, the energies of the deexcitation γ rays in the projectile frame were deduced to be 212(8) keV and 333(10) keV. These values are compatible with the earlier results [2,17]. The inset of Fig. 2 shows a Doppler-corrected spectrum of γ rays, which were obtained with the entire NaI(Tl) array by imposing coincidence with outgoing ^{17}C particles. In this spectrum covering a wider energy region one notices three notable peaks above the one neutron separation threshold of 730 keV. Among them two peaks between 1.5 and 1.8 MeV are ascribed to the 1585-keV and 1766-keV γ rays respectively due to the deexcitations of the first 2^+ states in the neighboring ^{16}C and ^{18}C nuclei [18], while the third peak around 2.3 MeV corresponds to the transition from the higher excited state(s) to the first 2^+ state in ^{16}C [18]. These γ rays in the neighboring isotopes were admixed into the ^{17}C spectrum due to the limitation of the mass separation by the hodoscope. We however note that the intensities of those γ rays are far weaker than those of the two peaks of ^{17}C so that the contaminant effects are hardly significant in the low-energy spectrum.

To deduce a full-energy-peak yield, a peak fitting procedure was applied, layer-by-layer, to the energy spectrum taken in the laboratory frame. The fitting function consisted of simulated spectra for the 212-keV and 333-keV γ rays folded on a background spectrum. This simulation for energy spectra involved effects of Doppler shift. Hence the information on the incoming and outgoing particles, such as the kinetic energy, the emittance, the energy loss in the target and the scattering angle was taken into account. The simulated spectra also depended on the position distribution of γ-ray emissions, hence the value of lifetime. In order to incorporate typical shapes of energy spectra, we thus performed the simulation using the τ values of 600 ps and 20 ps, respectively for the 212-keV and 333-keV γ rays, which are close to the final results in the present work. To fit the background spectrum we employed the shape of the energy spectrum obtained in coincidence with outgoing ^{14}C particles, which were produced by the break-up reaction of ^{18}C. This procedure appears to be reasonable since ^{14}C has no excited states up to 6 MeV emitting γ rays so that the low-energy part of the coincidence spectrum should be dominated by background contributions from beam-induced particles from the target, such as break-up neutrons or delta rays. The background component turned out to be very weak in the fitted spectrum.

The deficiencies (D_{exp}) for the γ rays from ^{17}C were then deduced for each layer of the NaI(Tl) array by using the full-energy-peak yields obtained for the data with and without the shield. Here, the differences of the integrated ^{18}C beam counts were corrected for. In Fig. 3, the D_{exp} values obtained for the center target position are plotted. The upper and lower panels respectively represent the results for the 212-keV and 333-keV states. In the case of the 333-keV state, the D_{exp} values were missing for the L5–L7 layers where the full-energy peaks were hardly seen in the spectra taken with the lead shield. To relate those D_{exp} values to the γ-decay lifetime, simulated values of deficiencies (D_{sim}) were obtained for varied values of lifetime. In the simulation using the GEANT code, isotropic γ-ray emissions were assumed in the deexcitations of excited nuclei. Fig. 3 shows the simulated deficiencies obtained for different values of τ, i.e., 400, 600 and 800 ps for the 212-keV state and 0, 20 and 50 ps for the 333-keV state. A quick comparison between the measured and simulated deficiencies indicates that the 212-keV state has a fairly long lifetime of about 600 ps, whereas the 333-keV state has a lifetime as short as 20 ps.

To determine lifetimes more precisely, a χ^2 analysis was employed. The χ^2 was defined as $\chi^2(\tau) = \sum_i (D^i_{\mathrm{exp}} - D^i_{\mathrm{sim}}(\tau))^2 / \Delta D^i_{\mathrm{exp}}{}^2$, where the summation index i runs over the layers. Here, the $D_{\mathrm{sim}}(\tau)$ stands for the simulated deficiency calculated with a given τ value. The ΔD_{exp} denotes the statistical error of the D_{exp} value. Note that in the present χ^2 analysis, we omitted the layers of which the D_{exp} values were missing. In the insets of Fig. 3, the $\chi^2(\tau)$ values are plotted as a function of τ, where the minimum χ^2 was determined from a parabolic function fitted to the

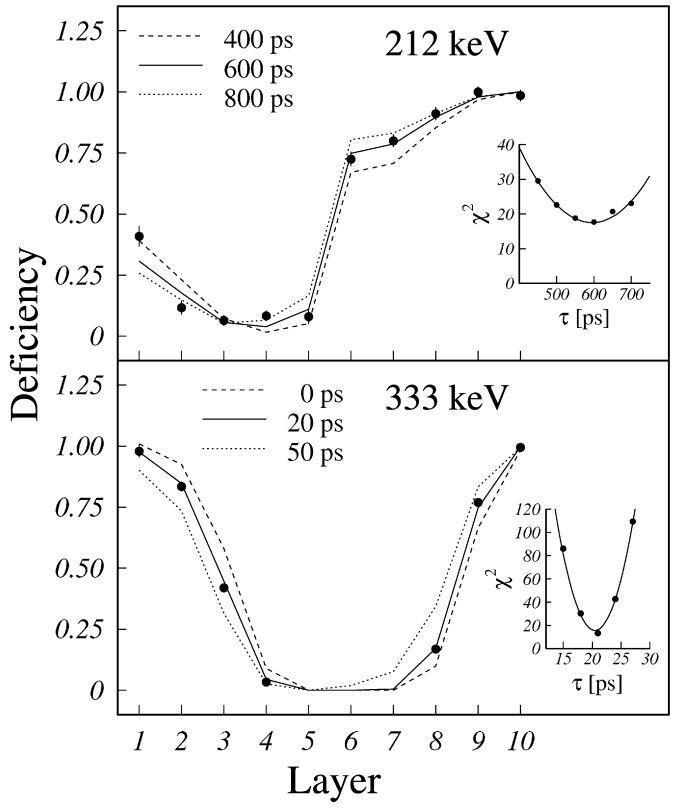

Fig. 3. The deficiencies obtained for the center target position. The upper (lower) panel shows the plot for the 212-keV (333-keV) γ rays. The data are shown by the solid circles and compared with the simulated deficiencies. The inset in each figure shows the χ^2 plot as a function of τ, together with the result of a fit using a parabolic function.

χ^2 plot. The mean lifetime of the 212-keV state was thus deduced to be 595(43) ps and 579(24) ps, respectively, for the center and the upstream target positions, while that of the 333-keV state was deduced to be 20.5(7) ps and 13.2(13) ps. By adopting weighted averages of these values, we obtain $\tau = 583(21)$ ps and 18.9(6) ps, respectively, for the 212-keV and 333-keV states. Here the numbers in the parentheses only represent the statistical errors, for which we assume the confidence level of one standard deviation.

As for the systematic errors, a major origin is attributed to the uncertainty of the target position, which was estimated to be ± 0.5 mm. This corresponds to a lifetime uncertainty of about ± 4.5 ps for outgoing ^{17}C particles with a mean velocity of $\beta \sim 0.38$. Another source is the ambiguity in the simulation. According to the calibration using the standard sources, the present simulation had an ambiguity of $\pm 3\%$ (or $\pm 7\%$) in reproducing the deficiency. To evaluate the uncertainty of the lifetime due to this ambiguity, we changed the $D_{\rm sim}$ randomly within the range of the estimated ambiguity and deduced the lifetimes. The resulting lifetimes changed within about $\pm 6\%$ and $\pm 8\%$, respectively, for the 212-keV and 333-keV states. By taking the root sum square of these two uncertainties, we obtained the total systematic errors of ± 35(syst) ps and ± 4.7(syst) ps, respectively, for the 212-keV and 333-keV states.

The validity of the present method was further tested by applying it to excited states with known lifetimes. We performed measurements on the 3^- state of ^{16}N at 298 keV and the $1/2^-$ state of ^{11}Be at 320 keV by populating these states in the ^{18}C+^{9}Be reaction. The mean lifetime of the 3^- state in ^{16}N was deduced to be $136 \pm 3(\text{stat})^{+11}_{-7}(\text{stat})$ ps, which is in good agreement with the known value of 132(2) ps [18]. For the case of ^{11}Be, the deduced mean lifetime was $4.6 \pm 1.1(\text{stat}) \pm 4.5(\text{syst})$ ps, which is consistent with the known short lifetime of 0.166(14) ps [18] within the error bar. However, the large error involved may imply that the present setup loses its sensitivity to lifetimes shorter than 10 ps. The details of the analysis on these two nuclei are described in Ref. [6].

The γ-decay lifetime can provide information on the multipolarity of the relevant transition. For the present case, the observed lifetimes are so short that the compatible multipolarities are limited to M1 or E1; namely, the E2 multipolarity is hardly possible since the E2 transition strengths corresponding to the lifetimes amount to the order of 10^3 Weisskopf units (W.u.), which far exceeds the upper limit of about 100 W.u. empirically observed for $A = 5$–44 nuclei [26]. Allowed multipolarity of the γ transition is further confined by the parities of the initial and final states involved. In the case of ^{17}C, only positive parity states are expected to appear below a few hundred keV because of large energy gaps between the *sd* shell and its neighboring shells. Indeed, the lowest negative parity states only appear at 3–4 MeV in the neighboring odd-neutron nuclei such as ^{15}C or ^{19}O. Since E1 transitions can only occur between states with opposite parities, we conclude that the observed γ decays in ^{17}C are dominated by M1 transitions. Predominance of M1 multipolarity is in harmony with the former spin-parity assignments of $5/2^+$ and $1/2^+$, respectively for the first and second excited states proposed in Refs. [2,19]. Assuming pure M1 transitions, the reduced M1 transition probabilities B(M1) to the ground state are deduced to be $(1.0 \pm 0.1) \times 10^{-2} \mu_{\rm N}^2$ for the 212-keV state and $(8.2^{+3.2}_{-1.8}) \times 10^{-2} \mu_{\rm N}^2$ for the 333-keV state. Note that the determination of the B(M1) generally requires the knowledge of the E2/M1 mixing ratio. In the present case, however, E2 contributions may be ignored since the change of B(M1) remains within the error bar even if the E2 strength is assumed to be as large as the empirical upper limit. In terms of Weisskopf unit, the B(M1) values for the 212-keV and 333-keV states, respectively, correspond to $(5.7^{+0.6}_{-0.5}) \times 10^{-3}$ W.u. and $(4.6^{+1.8}_{-1.0}) \times 10^{-2}$ W.u. We thus find that the former M1 transition is enormously hindered while hindrance of the latter is rather moderate.

In Fig. 4, we compare the low-lying level properties of ^{17}C with those of a stable $N = 11$ isotone, ^{21}Ne, which has a neutron emission threshold of as high as 6761 keV [18]. The lowest $1/2^+$, $3/2^+$ and $5/2^+$ states are shown together with their associated M1 transition strengths in the figure. For the first excited state of ^{17}C, we assume the tentative spin-parity assignment of Refs. [2,19]. In spite of the large difference of the binding energies, the comparison between these $N = 11$ isotones reveals several significant similarities, as primarily characterized by the common spin parity of $3/2^+$ for the ground states. Indeed the level properties of the $5/2^+$ states are remarkably similar between the two isotones; both the states are located at excitation energies of about 300 keV, being accompanied with almost identical M1 transition strengths to the respective ground states. On the other hand, very different appearances are highlighted in the comparison of the $1/2^+$ states; the excitation energy decreases dramatically from 2794 keV [18] for ^{21}Ne to 212 keV for ^{17}C. Furthermore, the associated M1 strength for ^{17}C is reduced by more than one order of magnitude as compared to that of ^{21}Ne. It is intriguing to note that the two low-lying excited states of $5/2^+$ and $1/2^+$ exhibit contradictory behaviors across the isotones of ^{21}Ne and ^{17}C, which implies a different nature of these ^{17}C states.

In order to infer the origins of these behaviors, we examine possible configurations of the low-lying states in terms of a naive Nilsson-model picture. As known from earlier studies [27–29], the low-lying states of ^{21}Ne have been well described with the Nilsson model assuming a large prolate deformation of $\beta \sim 0.3$. We then hope that arguments based on the same framework could provide

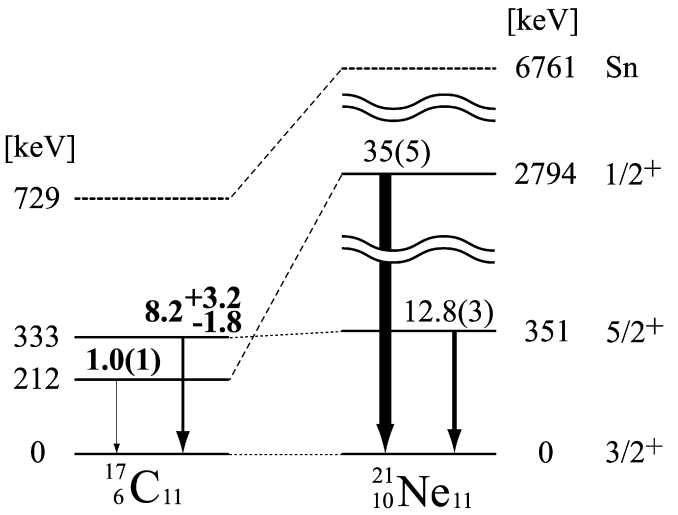

Fig. 4. The lowest $1/2^+$, $3/2^+$ and $5/2^+$ states in $N = 11$ isotones ^{17}C and ^{21}Ne. The values on the arrows represent the B(M1) value of the transition [$\times 10^{-2}\mu_N^2$]. The B(M1) values for the γ decays of the $5/2^+$ and $1/2^+$ states in ^{21}Ne are from Ref. [32] and Ref. [33], respectively.

useful hints about how the similarities and departures between ^{17}C and ^{21}Ne will arise.

According to the Nilsson model, prolate deformation promotes lowering of the [211]3/2 orbital down to the Fermi surface in a system of $N = 11$. This expectation is in harmony with the spin-parity assignments of $3/2^+$, which are experimentally established for the ground states of both the isotones. In the case of ^{21}Ne the low-lying $3/2^+$ and $5/2^+$ states are thus interpreted as members of the same rotational band built on the [211]3/2 orbital [27,28], well describing associated properties observed. As shown in Fig. 4 the locations of the $3/2^+$ and $5/2^+$ states as well as the connecting M1 strength are almost identical between the isotones of ^{17}C and ^{21}Ne. Hence it is probable that the ^{17}C states concerned can be as well ascribed to rotational band members of the [211]3/2 orbital, implying prevalence of deformation in ^{17}C. In fact this possibility is supported by the large deformation length observed for the relevant excitation in the proton inelastic scattering on ^{17}C [2].

As for the cases of the $1/2^+$ states, the ^{21}Ne state has been interpreted as the head of the rotational band built on the [211]1/2 Nilsson orbital [27,29]. For this orbital, admixture of $1d_{5/2}$ and $1d_{3/2}$ components is expected to increase as the prolate deformation is promoted [27]. As a matter of fact this feature is in harmony with the relatively large strength experimentally observed for the M1 transition to the ground state, where the d-wave neutron admixed in the [211]1/2 orbital is allowed to decay into the [211]3/2 orbital, which is solely comprised of the $1d_{5/2}$ and $1d_{3/2}$ components [27]. In this context we notice a unique situation for the $1/2^+$ state of ^{17}C that it is barely bound with a neutron separation energy of 0.52 MeV in contrast to the ^{21}Ne partner state with fairly sound binding of 3.97 MeV [18]. Such a loosely bound $1/2^+$ state tends to be subject to occurrence of halo structure, resulting in drastic change in wave function. Namely, in a nuclear state with extremely weak binding the component of $2s_{1/2}$ neutron will become more favored than the other components of higher orbital angular momenta since the former will gain more in the binding energy due to enhanced spatial extension involved [30,31]. One may thus anticipate appreciable increase of the $2s_{1/2}$ component in the [211]1/2 orbital in ^{17}C, reducing components of $1d_{5/2}$ and $1d_{3/2}$ neutrons. Naturally, the increased contribution of the $2s_{1/2}$ component should lead to the lowering of excitation energy for the $1/2^+$ state. Moreover, the altered configuration may cause considerable suppression of the M1 transition to the ground state, since the $2s_{1/2}$ component alone cannot connect via allowed M1 transition with the d-wave components which may be predominant for the ground state.

We have so far seen that qualitative features of the low-lying levels in ^{17}C may be roughly explained in terms of naive Nilsson schemes. It is particularly notable that the simple conjecture of the deformed [211]1/2 orbital with halo effects appears to afford a consistent account for the various anomalous features observed for the ^{17}C $1/2^+$ state. We however note that a mean-field calculation on ^{17}C indicated several local minima with rather shallow potentials, suggesting complexities involved in the collective phenomena of this isotone. The results of the present study are hence stimulating further studies on the exotic low-lying structure of ^{17}C from both experimental and theoretical sides.

In summary, the mean lifetimes of the first and second excited states of ^{17}C, respectively at 212 keV and 333 keV, were determined with the recoil shadow method to be $583 \pm 21(\text{stat}) \pm 35(\text{syst})$ ps and $18.9 \pm 0.6(\text{stat}) \pm 4.7(\text{syst})$ ps. Based on the electromagnetic strengths deduced, the observed deexcitations to the ground state were concluded to occur predominantly via M1 transitions, supporting spin-parity assignments of $1/2^+$ and $5/2^+$ for the first and second excited states proposed by earlier works. The B(M1) values were then deduced to be $(1.0 \pm 0.1) \times 10^{-2}\mu_N^2$ and $(8.2^{+3.2}_{-1.8}) \times 10^{-2}\mu_N^2$, respectively, for the 212-keV and 333-keV transitions. The M1 strength and excitation energy observed for the $5/2^+$ state are found to be very similar between ^{17}C and ^{21}Ne, suggesting prevalence of deformation in ^{17}C as well as in ^{21}Ne. On the other hand, the behavior of the $1/2^+$ state is found to be remarkably different in the two isotones. Naive Nilsson-model considerations support a conjecture that sizable reduction of M1 strength as well as the much lowered excitation energy characteristic of the ^{17}C $1/2^+$ state may be related to halo effects anticipated for a loosely bound deformed orbital.

Acknowledgements

We thank the RIKEN Ring Cyclotron staff members for providing a stable ^{22}Ne beam throughout the experiment. Fruitful discussions with Dr. M. Yamagami, Prof. T. Suzuki and Prof. I. Hamamoto are greatly appreciated. D.S. is grateful to the Japan Society for the Promotion of Science (JSPS) for scholarships. This work was supported in part by a Grant-in-Aid for Scientific Research No. 15204017 from JSPS.

References

[1] H.J. Ong, et al., Phys. Rev. C 73 (2006) 024610.
[2] Z. Elekes, et al., Phys. Lett. B 614 (2005) 174.
[3] N. Imai, et al., Phys. Rev. Lett. 92 (2004) 062501.
[4] Z. Elekes, et al., Phys. Lett. B 586 (2004) 34.
[5] M. Wiedeking, et al., Phys. Rev. Lett. 100 (2008) 152501.
[6] H.J. Ong, et al., Phys. Rev. C 78 (2008) 014308.
[7] Y. Kanada-En'yo, Phys. Rev. C 71 (2005) 014310.
[8] H. Sagawa, et al., Phys. Rev. C 70 (2004) 054316.
[9] T. Nakamura, et al., Phys. Rev. Lett. 83 (1999) 1112.
[10] J.P. Dufour, et al., Z. Phys. A 324 (1986) 487.
[11] H. Ueno, et al., Nucl. Phys. A 738 (2004) 211.
[12] D. Bazin, et al., Phys. Rev. C 57 (1998) 2156.
[13] T. Baumann, et al., Phys. Lett. B 439 (1998) 256.
[14] E. Sauvan, et al., Phys. Lett. B 491 (2000) 1.
[15] V. Maddalena, et al., Phys. Rev. C 63 (2001) 024613.
[16] U.D. Pramanik, et al., Phys. Lett. B 551 (2003) 63.
[17] M. Stanoiu, et al., Eur. Phys. J. A 20 (2004) 95.
[18] R.B. Firestone, V.S. Shirley, Table of Isotopes, vol. 1, 8th ed., Wiley, New York, 1996.
[19] H.G. Bohlen, et al., Eur. Phys. J. A 31 (2007) 279.
[20] T. Kubo, et al., Nucl. Instrum. Methods B 70 (1992) 309.
[21] H. Kumagai, et al., Nucl. Instrum. Methods A 470 (2001) 562.
[22] S. Takeuchi, et al., Phys. Lett. B 515 (2001) 255.
[23] S. Takeuchi, et al., RIKEN Accel. Prog. Rep. 36 (2003) 148.

[24] T. Nishio et al., RIKEN Accel. Prog. Rep. 29 (1996) 184.
[25] GEANT, CERN Program Library Long Writeup, W5013, 1994.
[26] P.M. Endt, At. Data Nucl. Data Tables 55 (1993) 171.
[27] A. Bohr, B.R. Mottelson, Nuclear Structure, vol. II, Benjamin, New York, 1975.
[28] C. Rolfs, et al., Nucl. Phys. A 167 (1971) 449.
[29] C. Rolfs, et al., Nucl. Phys. A 189 (1972) 641.
[30] M. Misu, et al., Nucl. Phys. A 614 (1997) 44.
[31] I. Hamamoto, Phys. Rev. C 69 (2004) R041306.
[32] R.B. Firestone, Nucl. Data Sheets 103 (2004) 269.
[33] E.K. Warburton, et al., Phys. Rev. C 20 (1979) 619;
E.K. Warburton, et al., Phys. Rev. C 23 (1981) 941, Erratum.